Available online at www.sciencedirect.com
SCIENCE DIRECT®
Journal of Pharmaceutical and Biomedical Analysis
33 (2003) 1117–1125
JOURNAL OF PHARMACEUTICAL AND BIOMEDICAL ANALYSIS
www.elsevier.com/locate/jpba

# Electrochemical detection of DNA immobilized on gold colloid particles modified self-assembled monolayer electrode with silver nanoparticle label

Meijia Wang [a,b], Chunyan Sun [b], Lianying Wang [a], Xiaohui Ji [a], Yubai Bai [a,*], Tiejin Li [a], Jinghong Li [b,*]

[a] College of Chemistry, Jilin University, Changchun 130021, PR China
[b] State Key Laboratory of Electroanalytical Chemistry, Changchun Institute of Applied Chemistry, Chinese Academy of Sciences, 159 People Street, Changchun 130022, PR China

Received 16 March 2003; received in revised form 15 July 2003; accepted 15 July 2003

**Abstract**

The target DNA was immobilized successfully on gold colloid particles associated with a cysteamine monolayer on gold electrode surface. Self-assembly of colloidal Au onto a cysteamine modified gold electrode can enlarge the electrode surface area and enhance greatly the amount of immobilized single stranded DNA (ssDNA). The electron-transfer processes of $[Fe(CN)_6]^{4-}/[Fe(CN)_6]^{3-}$ on the gold surface were blocked due to the procedures of the target DNA immobilization, which was investigated by impedance spectroscopy. Then single stranded target DNA immobilized on the gold electrode hybridized with the silver nanoparticle–oligonucleotide DNA probe, followed by the release of the silver metal atoms anchored on the hybrids by oxidative metal dissolution, and the indirect determination of the released solubilized $Ag^I$ ions by anodic stripping voltammetry (ASV) at a carbon fiber microelectrode. The results show that this method has good correlation for DNA detection in the range of 10–800 pmol/l and allows the detection level as low as 5 pmol/l of the target oligonucleotides.


*Keywords:* Colloidal Au; DNA; Self-assembled monolayer; Impedance spectroscopy; Silver nanoparticles label

## 1. Introduction

The development of DNA sensors attracts recent research efforts directed to gene analysis, identification of genetic disorders, tissue matching, and forensic application [1,2]. An electrochemical DNA biosensor is a novel and promising alternative method for sequence-specific DNA diagnosis and detection due to its advantages of being cheap, sensitive and rapid. With the development of electrochemical DNA biosensors, electrode surface-immobilization techniques for stable and highly dense single stranded DNA (ssDNA) monolayer become more important. There are many reported methods for surface-immobilizing

* Corresponding authors. Tel./fax: +86-431-526-2243.
*E-mail address:* lijingh@ciac.jl.cn (J. Li).

0731-7085/03/$ - see front matter © 2003 Elsevier B.V. All rights reserved.
doi:10.1016/S0731-7085(03)00411-4

ssDNA on the electrode surface, such as chemical adsorption [3,4], covalent-binding [5–8], the antigen–antiody interaction [9], electrostatic attraction [10–15] and co-polymerization [16]. DNA immobilization amounts on these electrodes were also reported. Surface densities of ssDNA with a mercaptohexyl group at the 5′-phosphate end on gold electrodes vary in the range of $1–4 \times 10^{13}$ molecules/cm$^2$ [17]. The detection limits of electrochemical DNA biosensors reported by several groups [9–15] were about $5 \times 10^{-9}$ mol/l. It is necessary to set up one new method to improve the sensitivity of electrochemical DNA biosensor.

Brossier [18] used a disposable electrochemical biosensor for the detection of DNA sequences related to the human cytomegalovirus (HCMV). Wang's team [19–22] described an electrochemical coding technology for the simultaneous detection of multiple DNA targets based on nanoparticle tags with diverse redox potentials. Such encoding nanoparticles thus offer a voltammetric signature with distinct electrical hybridization signals for the corresponding DNA targets. In this work, colloidal Au was used to enhance the DNA immobilization capacity on a gold electrode, and oligonucleotide-functionalized nanoparticles as probes provided a highly sensitive and selective detection format for DNA. In order to improve the sensitivity of $Ag^I$ ion detection, 15 μm diameter microelectrode, made of carbon fiber, and highly sensitive anodic stripping voltammetry (ASV) were employed. It was thus possible to achieve picomolar detection of the target oligonucleotides. We offer the opportunity to develop an inexpensive, simple, electrochemical detection way.

## 2. Experimental

### 2.1. Reagents

Chitosan oligomer (1.0% solution in 1.0% acetic acid) and sodium dodecylsulfate (SDS) were purchased from Sigma (USA). The following buffers were used: 0.1 mol/l PBS (0.1 mol/l NaCl+10 mmol/l sodium phosphate buffer, pH 7.0); 0.3 mol/l PBS (0.3 mol/l NaCl+10 mmol/l sodium phosphate buffer, pH 7.0); PB (4.3 mM $NaH_2PO_4$, 15.1 mM $Na_2HPO_4$, and 50 mM NaCl, pH 7.4); TE buffer (10 mmol/l Tris–HCl+1.0 mmol/l EDTA, pH 8.0). Trisodium citrate, $HAuCl_4$, KBr, $AgNO_3$, $NaBH_4$, $K_4Fe(CN)_6$, $K_3Fe(CN)_6$, and other reagents were commercially available analytical reagent grade.

The DNA used was purchased from Beijing **AuGCT** Biotechnology Co., Ltd. (Beijing, China).

target: 5′-SH-$(CH_2)_6$-ATACTGGCCGTCG-TATTACAACGTCGTGGT-3′;
probe: 5′-SH-$(CH_2)_6$-ACCACGACGTTG-TAATACGACGGCCAGTAT-3′;
one-mismatch containing sequences: 5′-SH-$(CH_2)_6$-ATACTGGCCGTCGTTTTA-CAACGTCGTGGT-3′.

All solutions were prepared with ultrapure water from a Millipore Milli-Q system.

### 2.2. Instrumental

UV–vis measurements were performed with a Cary 100 Spectrophotometer (VARIAN, USA) and optical wavelength range was selected from 300 to 700 nm.

Transmission electron microscopy (TEM) of Au nanoparticles was taken with a JEOL-JEM-2010 transmission electron microscope operating at 200 kV (JEOL, Japan). Samples for TEM were prepared by casting one drop of colloidal Au onto a standard carbon-coated (200–300 Å) formvar films on copper grid (230 mesh).

ASV measurements were carried out on a CHI 660 electrochemical analyzer (CHI Inc., USA), using a conventional three-electrode electrochemical cell. The electrodes were a carbon fiber microelectrode ($\Phi = 15$ μm), an Ag/AgCl (saturated KCl) reference electrode, and a Pt coil counter electrode. A macroscopic gold electrode ($\Phi = 2$ mm) was used for the target DNA immobilization and probe hybridization procedure. The AC-impedance measurements were performed with a Solartron 1470 Battery Test Unit and a Solartron 1255 B Frequency Response Analyzer (Solartron Inc., England) for 2.5 mM $K_4[Fe(CN)_6]$+2.5 mM $K_3[Fe(CN)_6]$ in 0.1 M $KNO_3$ and TE buffer (pH 8.0) solution. A

sinusoidal potential modulation of ±5 mV amplitude was superimposed on the formal potential of the redox couple of $[Fe(CN)_6]^{4-}/[Fe(CN)_6]^{3-}$ (0.22 V vs. Ag/AgCl). The impedance data were fitted to an electrical equivalent circuit using the ZPLOT/ZVIEW software (Scribner Associates Inc.). The equivalent circuit provides an electrical analogue of chemical/physical processes probed by AC-impedance measurements. Prior to the experiments, the electrolyte solutions were deoxygenated through bubbling with high-purity nitrogen for at least 20 min. All experiments were carried out at room temperature.

### 2.3. Preparation of Au colloids and Ag colloids

100 ml aqueous solution containing 0.1 mM $HAuCl_4$ and 0.15 mM trisodium citrate was prepared (here, trisodium citrate acted as a capping agent and thus restricted the growth of Au) [23]. Next, 1 ml of 0.05 M $NaBH_4$ solution was added at once into the gold solution under continuous stirring. Aqueous solution was then mixed and stirred vigorously for 2 h. Prepared Au colloid was stored in a dark glass bottle at 4 °C for further use.

Silver nanoparticles were prepared according to the literature [24] by sodium borohydride reduction of $AgNO_3$. Ice-cold $AgNO_3$ ($1 \times 10^{-3}$ mol/l) and equal volume of $NaBH_4$ ($3.0 \times 10^{-3}$ mol/l) were mixed dropwise, with stirring, in an ice-bath, continuously stirred while it was allowed to cool to room temperature. The solution was subsequently filtered through a cyclopore membrane (polycarbonate filter). The final silver nanoparticles prepared by this method have an average diameter of 25±3 nm as measured by transmission electron microscope.

### 2.4. Preparation of self-assembled monolayers (SAMs) of Au colloidal and immobilization of DNA on the gold electrode surface

The gold electrode was mechanically polished with 1, 0.3 and 0.05 μ $Al_2O_3$ and washed ultrasonically with double distilled water, subsequently electrochemically cleaned in 1 M $H_2SO_4$ by potential scanning between −0.2 and 1.55 V until a reproducible cyclic voltammogram was obtained. Then it was rinsed with copious amounts of double distilled water and dry ethanol in turn, finally blown dry with high-purity nitrogen before monolayer adsorption. The monolayers were formed through placing the clean bare gold electrode into a freshly made 0.1 M deoxygenated cysteamine aqueous solution for 2 h at room temperature in darkness. After adsorption, the gold electrode modified with cysteamine was thoroughly rinsed with double distilled water to remove physically absorbed cysteamine. Then the cysteamine modified electrode was dipped into an Au colloid solution ($5 \times 10^{-10}$ mol/l, pH 3.5) in darkness for 8 h at 4 °C to form Au colloidal modified electrode. The electrode was thoroughly rinsed using lot of double distilled water, subsequently blown dry with high-purity nitrogen. Finally, the Au colloid/systeamine/gold electrode was dipped into 1 ml of 0.3 mol/l phosphate buffer (pH 7.0) solution containing various concentrations of oligonucleotide at room temperature for 120 min, resulting in that ssDNA was immobilized on the colloidal Au-modified gold electrode. After thoroughly rinsing the electrode with 0.1% SDS phosphate buffer (pH 7.0), it was kept in a TE buffer (pH 8.0) at 4 °C. The immobilization processes of ssDNA onto the colloidal Au self-assembled monolayer modified gold electrode and the detection method of DNA are shown in Scheme 1.

### 2.5. Preparation of silver-nanoparticle-labeled oligonucleotide DNA probe and probe hybridization

Silver nanoparticle–oligonucleotide conjugates were synthesized by derivatizing 5 ml of silver nanoparticle solution with $8 \times 10^{-5}$ g 5′-mercaptohexyl-capped oligonucleotides. After standing for 20 h at room temperature, the pH and ionic strength of the solution were adjusted with phosphate buffer (0.08 mol/l, pH 7.4) and allowed to stand for other 6 h. Then, the total NaCl concentration of the solution was adjusted to 0.1 mol/l with NaCl. After an additional 72 h, the nanoparticles were isolated by centrifugation for 30 min at 12 000 rpm. The resulting DNA nanoparticle precipitate was washed with 0.1 mol/l PBS.

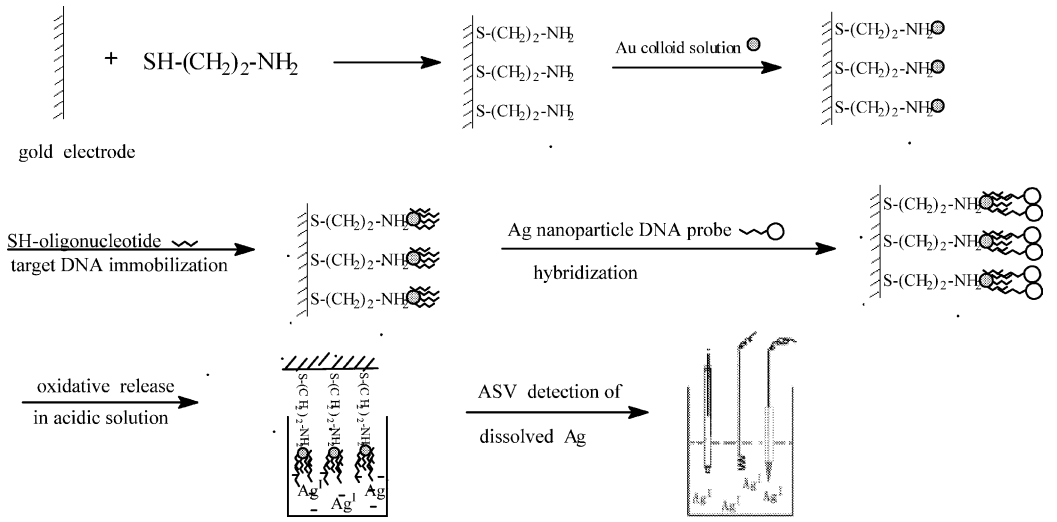


Scheme 1. The schematic illustration of the processes of the immobilization of DNA onto the gold electrode and detection by using Ag labeled complementary DNA.

The metal–oligonucleotide probe solution was stored at $-5\,^{\circ}C$. Different concentrations were prepared by diluting with 0.3 mol/l PBS solution.

The hybridization reaction was carried out by immersing the target DNA immobilized on the gold electrode in the prepared solution of silver-nanoparticle-labeled oligonucleotide DNA probe solution, and incubated at 37 °C for 60 min with nonstop shaking. After that, the electrode was washed three times with 0.1% SDS phosphate buffer (pH 7.0) to remove the unhybridized DNA probes.

### 2.6. Silver metal dissolution and electrochemical detection

The silver nanoparticles, which linked to the hybrids on the gold electrode surface, were dissolved by immersing the modified gold electrode in an analytical cell containing 200 μl of 50% $HNO_3$ solution for 10 min to ensure that the silver dissolution was completed [25]. After the gold electrode was removed, 100 μl of 0.1 M KBr and 200 μl of 0.1 M $KNO_3$ buffer were added into the cell, then the carbon fiber microelectrode (as the working electrode) was inserted into the cell. Reaction of the releasing $Ag^I$ ions with the $Br^-$ leads to the formation of the AgBr sedimentation, and then leads to the formation of the $[AgBr_2]^-$ with too much $Br^-$, which is easy to be detected by ASV. $Ag^I$ ions were cathodically electrodeposited at $-0.5$ V for 120 s, and immediately detected by anodic stripping (peak current $i_{p,a}$ at $+0.03$ V) at 50 mV/s. This analytical response is directly proportional to the amount of target DNA.

## 3. Results and discussion

### 3.1. Electrochemical characteristics of self-assembled monolayer of Au colloidal and DNA immobilization on the gold electrode

The diameter of the Au colloid was measured by UV–vis spectra and TEM image in Fig. 1. UV–vis spectroscopy showed an absorbance maximum at 505 nm and TEM micrograph showed that the average size of the Au colloid was about 6 nm [23].

On the gold electrode surface, the SAMs of chemisorbed cysteamine has been used as the base interface for the deposition of the Au colloid. It was believed that the thiol group of cysteamine bound to Au surface leaving the amine group free (in acid condition, here, pH 3.5) to bind with Au colloids introduced in solution.

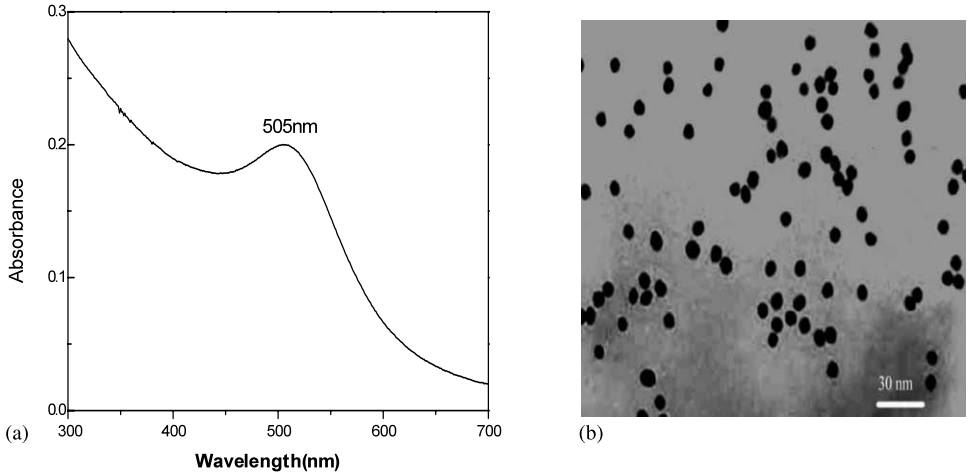


Fig. 1. UV–vis spectra of Au colloidal solutions (a) and TEM image of Au colloid (b).

Electrochemical impedance spectroscopy (EIS) can give information on the impedance changes of the electrode surface in the modification process. In EIS, the semicircle diameter of EIS equals the electron transfer resistance, $R_{ct}$, which controls the electron transfer kinetics of the redox-probe at the electrode interface. Complex impedance plots of 2.5 mM $K_4[Fe(CN)_6]$/2.5 mM $K_3[Fe(CN)_6]$ at bare gold electrode (a), cysteamine/gold electrode (b), Au colloid/cysteamine/gold electrode (c), target DNA/Au colloid/cysteamine/gold electrode (d) are shown in Fig. 2, and the corresponding equivalent circuit mold is shown in Scheme 2.

The semi-circle at the high frequencies represents the response of heterogeneous charge transfer kinetics. The relationships are given below [26,27]:

$$R_{ct} = RT/(nFi_o) \quad (1)$$

$$i_o = nFAk^oC \quad (2)$$

Herein, R, gas constant; T, room temperature; n, the electron transfer number of the redox couple, n = 1 as for $[Fe(CN)_6]^{4-}/[Fe(CN)_6]^{3-}$; F, Faraday constant; $i_o$, the exchange current between the gold electrode and the redox couple; A, the area of gold electrode; $k^o$, the charge transfer rate constant; C, the concentration of the redox couple. $k^o$ could be obtained from formula (1) and (2). The curve simulated by equivalent circuit is preferably close to the experimental impedance plot, which indicates that the equivalent circuit is accurate. The straight-line at the low frequencies is due to the

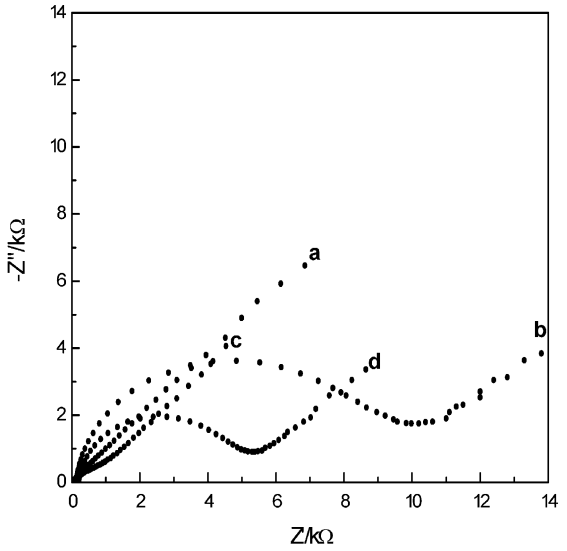


Fig. 2. Complex impedance plots of 2.5 mM $K_4[Fe(CN)_6]$/2.5 mM $K_3[Fe(CN)_6]$ at bare gold electrode (a), the SAMs of cysteamine/gold electrode (b), the monolayer of Au colloid/cysteamine/gold electrode (c), and target DNA/Au colloid/cysteamine/ gold electrode (d) in 0.1 M $KNO_3$ and TE buffer solution (pH 8.0). A sinusoidal potential modulation of $\pm 5$ mV amplitude was superimposed on the formal potential of the redox couple of $[Fe(CN)_6]^{4-}/[Fe(CN)_6]^{3-}$ (0.22 V vs. Ag/AgCl). Applied frequency was from $10^6$ to 0.1 Hz. Target DNA, 5′-SH-$(CH_2)_6$-ATACTGGCCGTCGTATTA-CAACGTCGTGGT-3′.

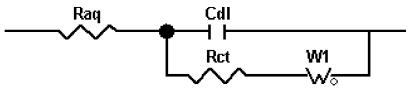


Scheme 2. Equivalent circuit mold for complex impedance plots. $R_{aq}$, solution resistance; $C_{dl}$, modified layer/solution interface capacitance; $R_{ct}$, charge transfer resistance due to electron transfer at the modified layer/solution interface; W1, Warburg diffusion impedance due to diffusion of the redox couple, ($[Fe(CN)_6]^{4-}/[Fe(CN)_6]^{3-}$), in the solution.

diffusion of the redox couple toward the gold electrode. The diameters of the semi-circle represent the resistance of the layers, which indicates their blocking behaviors for the electron-transfer processes of the redox couple at gold electrode. It is usually assumed that the electrode transfer of $[Fe(CN)_6]^{4-}/[Fe(CN)_6]^{3-}$ redox probe was blocked by formation of a highly organized layers on the electrode surface because these redox species do not penetrate the layers into the conductive electrode surface. The precipitate of $k^o$ as an electrical barrier could be reflected by the electron-transfer resistance of the redox probe of $[Fe(CN)_6]^{4-}/[Fe(CN)_6]^{3-}$. It can be seen from Fig. 2 that the bare gold electrode exhibits an almost straight line, one characteristic of a diffusion-limiting step of the electrochemical process. After being immersed in cysteamine aqueous solution, the EIS of the resulting assembled cysteamine monolayer showed a higher interfacial electron transfer resistance, for example $R_{ct}$, 9676 Ω and $k^o$, $3.50 \times 10^{-6}$ m/s in curve b, indicating that the highly organized cysteamine monolayer obstructed interfacial electron transfer of the electrochemical probe. Immersion of 6-nm Au colloidal on cysteamine SAMs modified electrode results in a visible decrease in the semicircle diameter, corresponding to a lower electron-transfer resistance at the electrode interface. We note that the semicircle of the monolayer of the Au colloid approaches an almost straight line similar to that of a bare gold electrode. This fast electrode-transfer kinetics originates from the enlarged surface areas of nano-Au colloidal layer. $R_{ct}$ of the semicircle in Fig. 2d increased to 5.1 kΩ, and $k^o$ diminished to $6.65 \times 10^{-6}$ m/s, indicating that the effective immobilization of target DNA on the Au colloidal monolayer.

The Au colloid modified gold electrode was dipped into 1 ml of 0.3 mol/l phosphate buffer (pH 7.0) solution containing various concentrations of oligonucleotide for 120 min at stir situation. At last, the electrode was thoroughly rinsed with 0.1% SDS phosphate buffer (pH 7.0) to remove physically adsorbed ssDNA. The complex impedance behaviors of 2.5 mM $K_4[Fe(CN)_6]$/2.5 mM $K_3[Fe(CN)_6]$ at the target DNA/Au colloid/cysteamine/gold electrode under the effect of the concentration of the immobilized target DNA are shown in Fig. 3. We note that the semicircle gradually become larger with an increase of the concentrations of oligonucleotide. The signal increases laggardly when target DNA concentration is above 800 ng/ml, this might be due to the saturated amount of target ssDNA immobilized on the surface of electrode. An independent set of

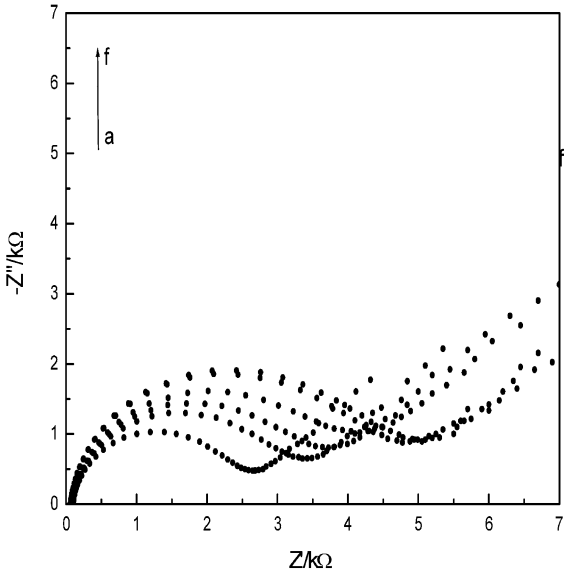


Fig. 3. The effect of target DNA immobilization amount on the complex impedance behaviors of 2.5 mM $K_4[Fe(CN)_6]$/2.5 mM $K_3[Fe(CN)_6]$ at the target DNA/Au colloid/cysteamine/gold electrode. Target DNA immobilization amount (pmol/l): (a) 10; (b) 150; (c) 300; (d) 500; (e) 650; (f) 800 and (g) 1000. Electrochemical probe, 2.5 mM $K_4[Fe(CN)_6]$/2.5 mM $K_3[Fe(CN)_6]$; solution, 0.1 M $KNO_3$ and TE buffer, pH 8.0. A sinusoidal potential modulation of ±5 mV amplitude was superimposed on the formal potential of the redox couple of $[Fe(CN)_6]^{4-}/[Fe(CN)_6]^{3-}$ (0.22 V vs. Ag/AgCl). Applied frequency was from $10^6$ to 0.1 Hz. Target DNA, 5′-SH-$(CH_2)_6$-ATACTGGCCGTCGTATTACAACGTCGTGGT-3′.

experiments showed that the saturated oligonucleotide surface coverage of 30-base oligonucleotide on a Au colloid-cysteamine-modified gold electrode was $2.67 \times 10^{14}$ molecules/cm$^2$. AC-impedance results for the DNA immobilization were listed in Table 1.

### 3.2. Detection of DNA hybridization involving a silver nanoparticle label

ASV has proved to be a very sensitive method for trace determination of metal ions [28]. In this analytical technique, the metal is cathodically electrodeposited onto the electrode surface during a preconcentration period ($t_{acc}$), and it is then stripped from the electrode by anodic oxidation. Electrodeposition potential ($E_d$), $-0.5$ V (vs. Ag/AgCl); Preconcentration period ($t_{acc}$), 120 s; scan rate, 50 mV/s. In this study, the detection of DNA hybridization was based on the fact that $Ag^I$ can be released completely under acidic condition and easily be detected by ASV as forming AgBr and $[AgBr_2]^-$.

In our report, the sample ssDNA was immobilized on the electrode surface and hybridized with sequence-known DNA probes, which are already labeled with an electrochemically active reagent, silver nanoparticles. Only complementary sample DNA can form a double-stranded DNA with the probes, and be diagnosed using electrochemical techniques. This is confirmed by comparing the difference of the electrochemical signal of the solubilized $Ag^I$ in the cases of one complementary oligonucleotide sequences (Fig. 4a) and one single mismatch oligonucleotide sequences (Fig. 4b). A well-defined Ag stripping signal (Ep = +0.03 V, vs. Ag/AgCl) was observed for the complementary sequence, which was significantly larger than that of the single-mismatch containing oligomer.

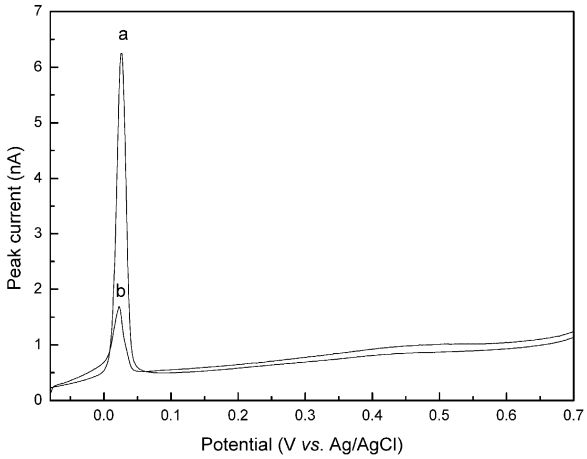


Fig. 4. The ASV response of dissolved silver at a 15 μm diameter carbon fiber working electrode. Electrodeposition potential ($E_d$), $-0.5$ V (vs. Ag/AgCl); Preconcentration period ($t_{acc}$), 120 s; scan rate, 50 mV/s. (a) complementary oligonucleotide sequences, 5′-SH-$(CH_2)_6$-ACCACGACGTTGTAATACGACGGCCAGTAT-3′; (b) oligonucleotide sequences containing a single-base mismatch, 5′-SH-$(CH_2)_6$-ATACTGGCCGTCGTTTTACAACGTCGTGGT-3′.

The use of a macroscopic Au colloid-cysteamine-modified gold electrode for oligonucleotide immobilization and hybridization, further to several rinses in buffer solution, efficiently separated the hybrid from the nonspecific adsorbate and non-hybridized DNA, thereby leading to a minimization of any nonspecific binding effects and the

Table 1
AC-impedance results to immobilization amount of target DNA on the modified electrode from Fig. 3

| Concentration of target DNA (pmol/l) | 10 | 150 | 300 | 500 | 650 | 800 | 1000 |
|---|---|---|---|---|---|---|---|
| $R_{ct}$ (Ω) | 1799 | 2610 | 3339 | 3742 | 4271 | 4924 | 5101 |
| $k^o$ ($10^{-6}$ m/s) | 18.8 | 12.9 | 10.15 | 9.06 | 7.94 | 6.88 | 6.65 |

$R_{ct}$, charge transfer resistance due to electron transfer at the modified layer/solution interface; $k^o$, charge transfer rate constant. The impedance measurements were carried out in the solution of 0.1 M $KNO_3$ and TE buffer (pH 8.0) solution. Electrochemical probe, 2.5 mM $K_4[Fe(CN)_6]$/2.5 mM $K_3[Fe(CN)_6]$. Modified electrode: target DNA/Au colloid/cysteamine/gold electrode. Target DNA, 5′-SH-$(CH_2)_6$-ATACTGGCCGTCGTATTACAACGTCGTGGT-3′. A sinusoidal potential modulation of ±5 mV amplitude was superimposed on the formal potential of the redox couple of $[Fe(CN)_6]^{4-}/Fe(CN)_6]^{3-}$ (0.22 V vs. Ag/AgCl). Applied frequency was from $10^6$ to 0.1 Hz.

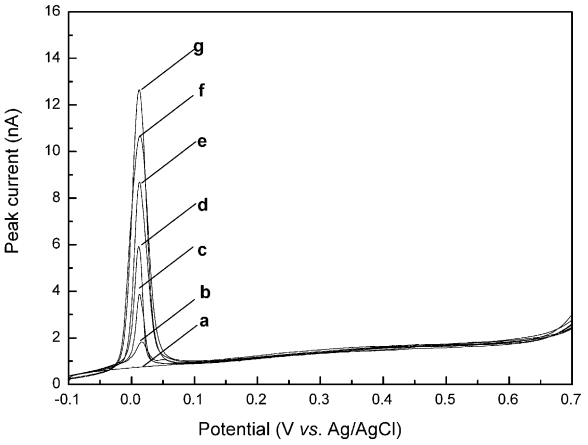


Fig. 5. The ASV response of dissolved silver at a 15 μm diameter carbon fiber working electrode, as a function of target DNA concentration. Electrodeposition potential ($E_d$), −0.5 V (vs. Ag/AgCl); Preconcentration period ($t_{acc}$), 120 s; scan rate, 50 mV/s. The target DNA concentration (pmol/l): (a) 0; (b) 10; (c) 150; (d) 300; (e) 500; (f) 650 and (g) 800.

ability to show good discrimination. As shown in Fig. 5, the electrochemical signal is directly proportional to the amount of analyte (target ssDNA). The sensitivity of the silver-nanopartical-based electrochemical hybridization assay was investigated by varying the target oligonucleotide concentration over the 2–1000 pmol/l range. The results show the linear response for the assay extended between 10 and 800 pmol/l, and allow the detection at levels as low as 5 pmol/l of the target oligonucleotides. The signal increased less when the target concentration was above 800 pmol/l. It might be due to the saturated amount of target DNA molecules.

## 4. Conclusions

In this report, Au colloidal electrodes were prepared by using cysteamine as cross-linkers, which have large surface area to increase the immobilization amount of ssDNA, and to monitor easily DNA hybridization. Our work combined Au nanoparticals films, ssDNA immobilization, silver nanoparticles labels, and EIS and electrochemical stripping analysis technology to monitor DNA hybridization. The results show that this method has good correlation for detection of ssDNA in the range of 10–800 pmol/l and allows detection at levels as low as 5 pmol/l of the target oligonucleotides. Thus, electrochemical gene analysis based on particle-labeled targets is a promising method as far as analytical sensitivity is concerned.

## Acknowledgements

This work was supported by 863 project, Outstanding Youth Fund (No. 20125513) from the National Scientific Foundation of China, 100 People Plan from Chinese Academy of Sciences and 100 outstanding Ph.D. thesis award of China.

## References

[1] E.A. Winzeler, D.R. Richards, A.R. Conway, A.L. Goldstein, S. Kalman, M.J. McCullough, J.H. McCusker, D.A. Stevens, L. Wodicak, D.J. Lockhart, R.W. Davis, Science 281 (1998) 1194–1197.
[2] S.R. Mikkelsen, Electroanalysis 8 (1996) 15–19.
[3] L. Hannah, V. Vetterl, Bioelectrochem. Bioenerg. 46 (1998) 7–13.
[4] D.W. Pang, M. Zhang, Z.L. Wang, J. Electroanal. Chem. 403 (1996) 183–188.
[5] Y.D. Zhao, D.W. Pang, S. Hu, Z.L. Wang, J.K. Cheng, H.P. Dai, Talanta 49 (1999) 751–758.
[6] K.M. Millan, A. Saraullo, S.R. Mikkalsen, Anal. Chem. 66 (1994) 2943–2948.
[7] S.H. Liu, C.L. Sun, P.G. He, Y.Z. Fang, Chin. J. Anal. Chem. 27 (1999) 130–134.
[8] X.Y. Sun, P.G. He, S.H. Liu, J.N. Ye, Y.Z. Fang, Talanta 47 (1998) 487–495.
[9] S. Palanti, G. Marrazza, M. Mascini, Anal. Lett. 29 (1996) 2309–2331.
[10] J. Wang, X.H. Cai, G. Rivas, H. Shiraishi, P.A.M. Farias, N. Dontha, Anal. Chem. 68 (1996) 2629–2634.
[11] J. Wang, G. Rivas, X.H. Cai, N. Dontha, H. Shiraishi, D.B. Luo, F.S. Valera, Anal. Chim. Acta 337 (1997) 41–48.
[12] G. Marrazza, I. Chianella, M. Mascini, Anal. Chim. Acta 387 (1999) 297–307.
[13] G. Marrazza, I. Chianella, M. Mascini, Biosens. Bioelectron. 14 (1999) 43–51.
[14] A. Erdem, K. Kerman, B. Meric, U.S. Akareca, M. Ozsoz, Electroanalysis 11 (1999) 586–591.

[15] J. Labuda, M. Buckowva, M. Vanickova, J. Mattusch, R. Wennrich, Electroanalysis 11 (1999) 101–107.
[16] C. Xu, H. Cai, P.G. He, Y.Z. Fang, Fresenius' J. Anal. Chem. 369 (2001) 428–432.
[17] A.B. Steel, R.L. Levicky, T.M. Herne, M.J. Tarlov, Biophys. J. 79 (2000) 975–981.
[18] F. Azek, C. Grossiord, M. Joannes, B. Limoges, P. Brossier, Anal. Biochem. 284 (2000) 107–113.
[19] J. Wang, R. Polsky, D. Xu, Langmuir 17 (2001) 5739–5741.
[20] J. Wang, D. Xu, R. Polsky, A. Kawde, Anal. Chem. 73 (2001) 5576–5581.
[21] J. Wang, G. Liu, R. Polsky, Electrochem. Commun. 4 (2002) 819–823.
[22] J. Wang, A. Kawde, M. Musameh, G. Rivas, Analyst 127 (2002) 1279–1282.
[23] V. Patil, R.B. Malvankar, M. Sastry, Langmuir 15 (1999) 8197–8206.
[24] J.A. Creighton, C.G. Blatchford, M.G. Albrecht, J. Chem. Soc., Faraday Trans. 275 (1979) 790–798.
[25] H. Cai, Y. Xu, N.N. Zhu, P.G. He, Y.Z. Fang, Analyst 127 (2002) 803–808.
[26] E. Sabatani, I. Rubinstein, J. Phys. Chem. 91 (1987) 6663–6669.
[27] I. Rubinstein, J. Rishpon, S. Gottesfeld, J. Electrochem. Soc. 133 (1986) 729–734.
[28] P.M. Bersier, J. Howell, C. Bruntlett, Analyst 119 (1994) 219–232.